Modelling and Simulation of High-viscosity, Non Iso-thermal Fluids with a Free Surface

Dimitri Harder, Edmond Skeli and Dirk Weidemann
Institute of System Dynamics and Mechatronics, University of Applied Sciences Bielefeld, Bielefeld, Germany

Keywords: Navier-Stokes, Differential-Algebraic Equation, Marker and Cell, Fluid Simulation, Free Surface.

Abstract: With the aim of using efficient control and/or diagnostic methods, more and more companies in the process engineering industry are using mathematical models to describe the underlying physical processes in sufficient detail. Against this background, the modeling and simulation of the behaviour of a non-isothermal, highly viscous fluid flow is examined in this paper. The behaviour of the fluid is decribed by a system of partial differential equations, which includes the incompressible Navier-Stokes equations as well as the thermal energy equation. With regard to the numerical calculation of the process variables, a combination of the Marker and Cell (MAC) method and a temperature calculation on a curvilinear grid is presented. The MAC method is used to identify the free surface by inserting particles without masses over the initialized fluid area and moving them with the calculated velocities. A characteristic feature of the typical use of the MAC method is that the defining partial differential equations are discretized spatially on a rectangular grid. However, this leads to the problem that a large part of the grid nodes lies within the obstacles which are surrounded by the fluid. In the present model, on the other hand, a curvilinear grid is used. The main advantage of this is that the outer grid nodes lie directly on the surrounding obstacles, resulting in a reduced system of differential-algebraic equations.

1 INTRODUCTION

The subject of this paper is the modelling and simulation of a non-isothermal, highly viscous fluid which enters between two counter-rotating cylinders. At the beginning there is no fluid between the cylinders. This space is filled with fluid only when entering. The entry of the fluid is an unsteady process in which the position of the fluid free surface changes over time. With regard to the determination of fluid behavior, knowledge of the temporal change of the fluid surface is important. Harlow and Welch (Harlow and Welch, 1965) first introduced a technique to calculate the time-dependent incompressible Navier-Stokes equations with a free surface, the Marker and Cell (MAC) method. Amsden and Harlow (Amsden and Harlow, 1970) simplified the MAC method by decoupling the speed from the pressure calculation. The works of (Tome et al., 2000; McKee et al., 2008) describe the MAC method in three-dimensional space. An overview of other methods for determining a free surface area can be found in the literature (Weston, 2000).

In contrast to the flow models of the literature listed above, models in control systems are expressed in state-space form. For such models, however, the number of states is kept small in order to realize efficient control and/or diagnostic methods (Jones et al., 2015). For control models, there is a balance between reducing complexity and increasing model uncertainty. Since linearized models are commonly used in control models, numerous studies have been carried out which linearize the Navier-Stokes equations around a chosen steady state flow condition (Jovanovic and Bamieh, 2001; Dellar and Jones, 2016; Aamo and Krstic, 2003). All these models resemble that they are considered in a closed fluid space, in other words, the presence of a free surface in such models has not yet been taken into account. This complicates the model by the state of a free surface.

In this paper the focus is on the nonlinear Navier-Stokes equations and a reduction of the dimension of the differential-algebraic system (DAE-system), which we obtain after a suitable spatial discretization. In the model, a curvilinear grid is used instead of a rectangular grid. The main advantage of the curvilinear grid is that the outer nodes are located on the surface of the cylinders, while the outer nodes of the rectangular grid are located inside the cylinders. Thus,

Harder, D., Skeli, E. and Weidemann, D.
Modelling and Simulation of High-viscosity, Non Iso-thermal Fluids with a Free Surface.
DOI: 10.5220/0006857405570563
In *Proceedings of the 15th International Conference on Informatics in Control, Automation and Robotics (ICINCO 2018) - Volume 2*, pages 557-563
ISBN: 978-989-758-321-6

the resulting DAE-system using a curvilinear grid has a lower dimension than the rectangular grid. In addition, the determination of the free surface area plays an important role. Therefore, the model presented here is based on a flow model rather than a fluid control model, however, the model is to be used as a basis for the further development of a control model. In addition to pressure and velocity, the temperature of the fluid is also determined.

The paper is structured as follows: In section 2 the partial differential-algebraic equations (PDAE) describing the behaviour of the fluid are given. Section 3 deals with the spatial discretization of the PDAE and the structure of the resulting DAE-system. Section 4 explains the solution procedure. The determination and setting of the boundary conditions of the free surface is described in section 5. This is followed by the temperature results in section 6.

2 MODELLING

The Navier-Stokes equations represent the dynamics of the fluid. In addition, the thermal energy describes the temperature behaviour. In the present case, the behaviour of the incompressible fluid in two-dimensional space without the influence of gravity, which is negligible due to its high viscosity, is considered and can be described as

$$\frac{\partial u}{\partial t}+u\frac{\partial u}{\partial x}+v\frac{\partial u}{\partial y}=-\frac{1}{\rho}\frac{\partial p}{\partial x}+\frac{\eta}{\rho}\left(\frac{\partial^2 u}{\partial x^2}+\frac{\partial^2 u}{\partial y^2}\right), \quad (1)$$

$$\frac{\partial v}{\partial t}+u\frac{\partial v}{\partial x}+v\frac{\partial v}{\partial y}=-\frac{1}{\rho}\frac{\partial p}{\partial y}+\frac{\eta}{\rho}\left(\frac{\partial^2 v}{\partial x^2}+\frac{\partial^2 v}{\partial y^2}\right), \quad (2)$$

$$0=\frac{\partial u}{\partial x}+\frac{\partial v}{\partial y}. \quad (3)$$

with initial and boundary conditions:

$$\mathbf{u}(\zeta,0)=\mathbf{u}_0(\zeta), \quad \forall\zeta\in\Gamma$$

$$\mathbf{u}(\zeta,t)=\mathbf{h}(\zeta,t), \quad \forall(\zeta,t)\in\partial\Gamma\times[0,t_e]$$

where u, v denotes the velocity components in x, y direction, respectively. Thus, the velocity vector is $\mathbf{u}=(u,v)^T:\Gamma\times\mathbb{R}_{(+)}\to\mathbb{R}^d$, where d is the spatial dimension (here $d=2$), $\mathbf{u}_0(\zeta)\in\mathbb{R}^2$ and $\mathbf{h}:\partial\Gamma\times\mathbb{R}_{(+)}\to\mathbb{R}^2$ denotes the vectors of initial and boundary conditions, respectively, $p:\Gamma\times\mathbb{R}_{(+)}\to\mathbb{R}$ is the pressure, $\rho\in\mathbb{R}$ the density, $\eta\in\mathbb{R}$ the dynamic viscosity of the fluid, $t\in[0,t_e]$ is the time and $t_e\in\mathbb{R}_{(+)}$ is the endpoint of the time interval. The considered domain of fluid flow is $\Gamma\subset\mathbb{R}^d$, with domain boundary $\partial\Gamma$ and inthere located points $\zeta\in\Gamma$.

Furthermore, the time and local development of the temperature T is described by the following partial differential equation

$$\rho C_p\left(\frac{\partial T}{\partial t}+u\frac{\partial T}{\partial x}+v\frac{\partial T}{\partial y}\right)= \lambda\left(\frac{\partial^2 T}{\partial x^2}+\frac{\partial^2 T}{\partial y^2}\right) +2\eta\left(\frac{\partial u}{\partial x}\right)^2+\eta\left(\frac{\partial u}{\partial y}+\frac{\partial v}{\partial x}\right)^2+2\eta\left(\frac{\partial v}{\partial y}\right)^2, \quad (4)$$

where $T:\Gamma\times\mathbb{R}_{(+)}\to\mathbb{R}$ represents the temperature within the domain Γ and $C_p,\lambda\in\mathbb{R}$ are the specific heat capacity and heat conductivity of fluid. The initial and boundary conditions are

$$T(\zeta,0)=T_0(\zeta), \quad \forall\zeta\in\Gamma$$

$$T(\zeta,t)=d(\zeta,t), \quad \forall(\zeta,t)\in\partial\Gamma\times[0,t_e]$$

where $T_0(\zeta)\in\mathbb{R}$ and $d\in\mathbb{R}$ includes the initial and boundary conditions, respectively.

3 SPATIAL DICRETIZATION

A known procedure for determining the local shape of a free surface on fluids is the MAC method, see (Amsden and Harlow, 1970; Tome and McKee, 1994) and the explanations in section 5. In order to use the MAC method, it is necessary to calculate the velocities of the fluid and thus solve the underlying Navier-Stokes equations. With regard to a numerical solution of the Navier-Stokes equations, it is necessary to convert the partial differential-algebraic system into a DAE-system, which can be achieved with a suitable spatial dicretization. The relevant process variables, such as velocity, pressure and the temperature are computed with a staggered grid. The components of velocity are calculated according to the representation in Fig. 1 in the middle of the cell edges and the pressure and temperature caculated in the middle of the cells. A cell is thus defined by the edges at which the velocities are calculated.

If the differentials are transferred to Taylor rows locally with the help of the Taylor polynomial and simplified accordingly, the following differential operators are obtained (Hou and Wetton, 1993):

$$D^x f_{i,j}=\frac{f_{i,j+1}-f_{i,j-1}}{2\Delta x} \quad \text{(centered)}, \quad (5)$$

$$D^x_- f_{i,j}=\frac{f_{i,j}-f_{i,j-1}}{\Delta x} \quad \text{(backward)}, \quad (6)$$

$$D^x_+ f_{i,j}=\frac{f_{i,j+1}-f_{i,j}}{\Delta x} \quad \text{(forward)} \quad (7)$$

and for the 2nd order center difference approximation which can be wirtten as follows:

$$K^x f_{i,j}=\frac{f_{i,j+1}-2f_{i,j}+f_{i,j-1}}{(\Delta x)^2} \quad (8)$$

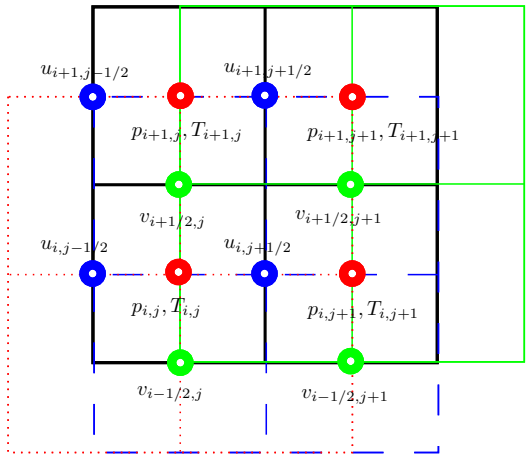

Figure 1: Staggered grid with the calculation nodes.

where $n_1, n_2 \in \mathbb{R}$ denotes the number of discretisation lines in x and y direction, respectively and $i = 1,2,...,n_1$ and $j = 1,2,...,n_2$ are the indices of the cells. f represents any of considered variables on certain node of the grid, which will be treated through the corresponding operator listed above and Δx is the discretisation step in x direction. In y-direction we define the operators D^y, D^y_-, D^y_+ and K^y similarly. With these operators we can discrete our PDAE-system (1) - (4) and we get the equations

$$I\dot{\mathbf{u}}(t) = K(\mathbf{u})\mathbf{u}(t) - Bp(t) + \mathbf{f}(\mathbf{u}(t), p(t)) \quad (9)$$

$$0 = B^T\mathbf{u}(t) \quad (10)$$

$$I\dot{T}(t) = K_1(\mathbf{u})T(t) + D(\mathbf{u}) + g(T(t)), \quad (11)$$

where I is the identity matrix, $B = [D^x_+, D^y_+]^T$ is the discrete divergence operator and $K(\mathbf{u}) = (K + N(\mathbf{u}))$, with $K = [K^x, K^y]^T$ representing the linear (difusion) and

$$N(\mathbf{u}) = \begin{bmatrix} u_{i,j+1/2}D^x + v^*_{i,j+1/2}D^y \\ u^*_{i+1/2,j}D^x + v_{i+1/2,j}D^y \end{bmatrix}$$

representing the nonlinear (convection) terms. The velocity $u^*_{i+1/2,j}$ and $v^*_{i,j+1/2}$ are average velocities defined by the four velocities around the point $v_{i+1/2,j}$ or $u_{i,j+1/2}$:

$$u^*_{i+1/2,j} = \frac{1}{4}\left(u_{i,j-1/2} + u_{i,j+1/2} + u_{i+1,j+1/2} + u_{i+1,j-1/2}\right)$$

$$v^*_{i,j+1/2} = \frac{1}{4}\left(v_{i-1/2,j} + v_{i+1/2,j} + v_{i+1/2,j+1} + v_{i-1/2,j+1}\right)$$

The forcing functions $\mathbf{f}(\mathbf{u}(t), p(t))$ and $g(T(t))$ in the equations (9) and (11) comes from the boundary conditions. The operator $K_1(\mathbf{u}) = (K + N_1(\mathbf{u}))$ for the temperature calculation has the convection term $N_1(\mathbf{u})$ this can by described by:

$$N_1(\mathbf{u}) = \begin{bmatrix} \frac{u_{i,j-1/2}+u_{i,j+1/2}}{2}D^x \\ \frac{v_{i-1/2,j}+v_{i+1/2,j}}{2}D^y \end{bmatrix}$$

The Term $D(\mathbf{u})$ is defined by

$$D(\mathbf{u}) = 2\eta((D^x_+u)^2 + \frac{1}{\eta}(D^y_+u + D^x_+v)^2 + (D^y_+v)^2).$$

With these presented discrete operators we receive the equations (9) - (11).

In Fig. 2 it is to be taken that the use of a rectangular grid causes individual grid points to be located outside the fluid area.

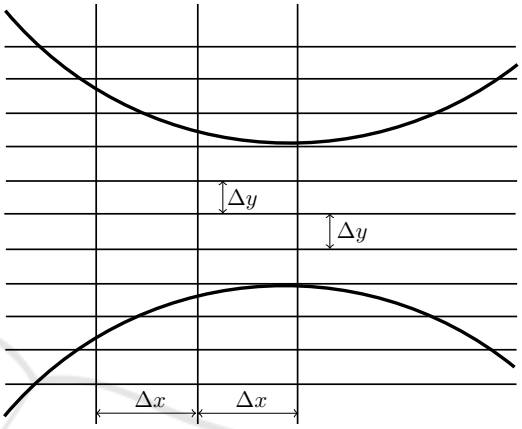

Figure 2: Rectangular equidistant grid.

With this background, a curvilinear grid is used in this case, where the step size Δx is constant, while Δy is varied along the flow direction, see Fig. 3. Analogous to the rectangular grid, the calculation points for the velocities are located at the center of the cell edge and the points for pressure and temperature at the center of the cell. Comparing both different grids and assuming a constant number of cells at the narrowest gap, e.g. four cells (as in Fig. 2 and 3. represented), results a higher dimensioned DAE-System from rectangular grid than using curvilinear grid. For example in our case we get for the identity matrix for the rectangluar grid $I_{rec} \in \mathbb{R}^{78\times50}$ and for the curvilinear grid $I_{cur} \in \mathbb{R}^{5\times50}$. The main advantage of a curvilinear grid is therefore a lower calculation effort. However, a sensible use of the curvilinear grid is only possible with sufficiently large radii, since there is the risk of an inaccurate calculation with small radii.

4 SOLUTION PROCEDURE

In order to solve the Navier-Stokes equations (9) - (10) on the basis of the Finite-Difference-Method (FDM), a pressure correction method, the projection method based on Chorin (Chorin, 1968) is used. The projection method is as follows (Weickert, 1996)

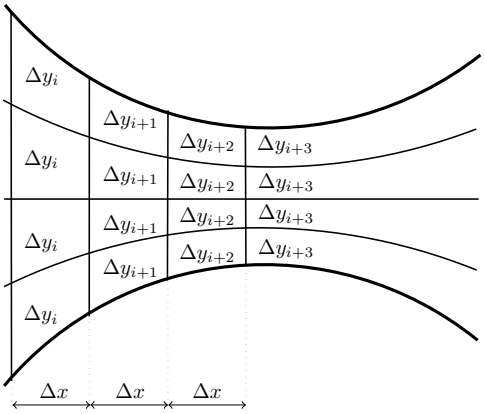

Figure 3: Curvilinear grid.

- Perform a semi-implicit time discretiziation with Δt as time discretization parameter and $n+1$ as the number of the current time step:

$$\frac{\mathbf{u}^{n+1}-\mathbf{u}^n}{\Delta t} = K(\mathbf{u}^n)\mathbf{u}^n - Bp^{n+1} + \mathbf{f}^{n+1} \tag{12}$$

$$0 = B^T\mathbf{u}^{n+1} \tag{13}$$

- Decouple the pressure from the momentum equation (12) and calculate the pseudo velocities $\tilde{\mathbf{u}}$ from the equation (14)

$$\frac{\tilde{\mathbf{u}}-\mathbf{u}^n}{\Delta t} = K(\mathbf{u}^n)\mathbf{u}^n + \mathbf{f}^{n+1} \tag{14}$$

$$\frac{\mathbf{u}^{n+1}-\tilde{\mathbf{u}}}{\Delta t} = -Bp^{n+1} \tag{15}$$

- Applying the dicrete divergence operator B on (15) we obtain the Poisson equation (16) and the equation for $\mathbf{u}^{n+1}$

$$\Delta t B^T B p^{n+1} = B^T\tilde{\mathbf{u}} \tag{16}$$

$$\mathbf{u}^{n+1} = \tilde{\mathbf{u}} - \Delta t B p^{n+1} \tag{17}$$

This strategy can be described by the strangeness free DAE-system (Weickert, 1996)

$$\begin{bmatrix} I & 0 \\ 0 & 0 \end{bmatrix}\begin{bmatrix} \dot{\mathbf{u}} \\ \dot{p} \end{bmatrix} = \begin{bmatrix} K(\mathbf{u}) & 0 \\ -B^T & \Delta t B^T B \end{bmatrix}\begin{bmatrix} \mathbf{u} \\ p \end{bmatrix} + \begin{bmatrix} \mathbf{f} \\ 0 \end{bmatrix}.$$

The temperature is calculated from (11) with the corrected speed values. The free surface is then determined.

5 DETERMINATION OF THE FREE SURFACE

The MAC method used here is found in the essays (Amsden and Harlow, 1970; Tome and McKee, 1994) and is used for determining the free surface. Massless particles are used to mark those cells that are partially or completely filled by the fluid. In other words, each cell in which includes at least one massless particle is part of the area in which the fluid is located. Against this background, the massless particles are also called markers. If there are empty cells border on a fluid cell, then this fluid cell is the one where the free surface passes. Such constellations are shown in Fig. 4 and 5. On a free surface for incompressible fluids, normal and tangential stresses are equal to zero, cf. (Hirt and Shannon, 1968; Nichols and Hirt, 1971). For a two-dimensional surface, the two following conditions apply

$$\frac{p}{\rho} - 2\frac{\eta}{\rho}\left[n_x n_x \frac{\partial u}{\partial dx} + n_x n_y\left(\frac{\partial u}{\partial y}+\frac{\partial v}{\partial x}\right) + n_y n_y \frac{\partial v}{\partial y}\right] = 0, \tag{18}$$

$$\left[2n_x m_x \frac{\partial u}{\partial x} + (n_x m_y + n_y m_x)\left(\frac{\partial u}{\partial y}+\frac{\partial v}{\partial x}\right) + 2n_y m_y \frac{\partial v}{\partial y}\right] = 0, \tag{19}$$

where $\mathbf{n} = (n_x, n_y)$ is the outward-looking normal and $\mathbf{m} = (m_x, m_y) = (n_y, -n_x)$ is the tangential vector.

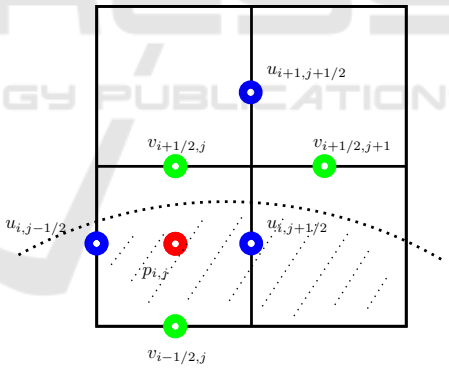

Figure 4: Marked cell with a free adjacent cell.

The free surface conditions are determined by the adjacent free cells, which is explained below using two examples. In Fig. 4 the lower left cell has one side bordering on a free cell. In this example, the normal component n_x is very small and (18) and (19) can be discretized and simplified to

$$p_{i,j} - 2\eta\left(D_+^y v\right) = 0, \tag{20}$$

and

$$D_+^y u = -D_+^x v$$

$$\frac{u_{i+1,j+1/2}-u_{i,j+1/2}}{\Delta y_{i,j+1/2}} = -\frac{v_{i+1/2,j+1}-v_{i+1/2,j}}{\Delta x} \tag{21}$$

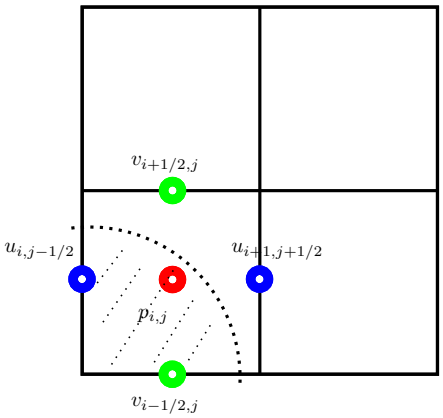

Figure 5: Marked cell with two free adjacent cells.

The pressure $p_{i,j}$ for the cell in Fig. 4 is calculated from (20) and the speed $u_{i+1,j+1/2}$ is calculated from (21), whereby the free surface conditions are fulfilled. Other scenarios, in which the selected cell borders on only one side of an empty cell, are simplified in the same way. In Fig. 5 two empty cells adjacent on the fluid cell, in such a scenario it is assumed that the normal vector points at an angle of 45° to the open sides. In this case (18) and (19) are simplified to

$$p - \eta \left(D_+^y u + D_+^x v \right) = 0 \tag{22}$$

and

$$D_+^x u - D_+^y v = 0. \tag{23}$$

In Fig. 5 the pressure is calculated based on (22) and the speeds $u_{i+1,j+1/2}$ and $v_{i+1/2,j}$ are equal to the opposite speeds of the fluid cell, so that (23) is fulfilled. Further scenarios, which can occur, can be found e. g. in (Amsden and Harlow, 1970; Tome and McKee, 1994).

6 RESULTS

Although the numerical results include the local and temporal course of the velocities, pressures and temperatures of the fluid, only individual temperature profiles of the fluid along the flow direction of three different layers at four different points in time are shown below. The temperature at time t_1, in all figures corresponds to the initialized area of fluid. The initialized temperature of the fluid is 425 Kelvin and the ambient temperature is 400 Kelvin. In Fig. 6 the fluid is attached to a cylinder with a constant temperature of 435 Kelvin. As the fluid moves forward as a result of cylinder rotation, the fluid is entering the gap. The change of pressure gradient due to the narrowing of the space between the cylinders, couses the acceleration respectiveley the deceleration of the different fluid layers. This leads to shearing of the fluid thus in an increase of temperature, so that the fluid partially assumes temperatures higher than the cylinder temperature. From the point where the shear decreases, the cylinder thus contributes to the cooling of the hotter fluid. The temperature profile at time t_4 shows in Fig. 6 also a shift to the right. This indicates that the fluid has flowed through the gap between the cylinders.

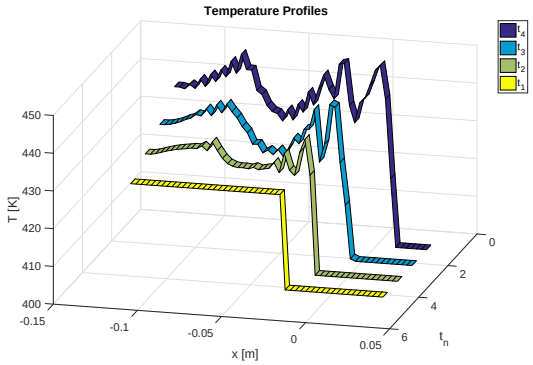

Figure 6: Temperature profiles of the layer adjacent to the upper cylinder.

The change in the temperature profile of the middle and the layer adjacent to the lower cylinder, see Fig. 7 and 8, is based on the same physical processes (shear, etc.) that have caused the temperature change of the layer adjacent to the upper cylinder.

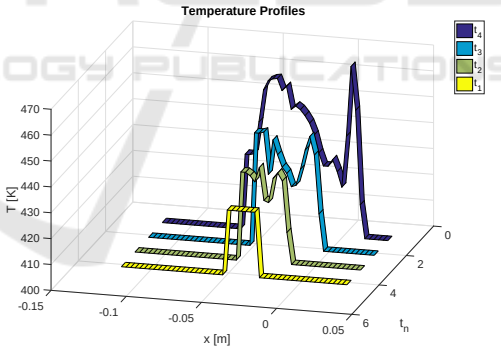

Figure 7: Temperature profiles of the middle layer.

In the Fig. 8 you can also see that the fluid in individual areas not only moves in the direction of the cylinder gap but also accumulates in individual places.

In Fig. 9 it can be seen that with a decreasing cylinder radius from one point upwards there is a significant deviation in the resolution of the velocity compared to the rectangular grid. This is partly due to the fact that small radii lead to increased curvature radii and thus in some places there are too large step widths in the y-direction and this causes numerical errors.

Fig. 10 shows the normalized calculation time between the grids required for 100000 time steps. As

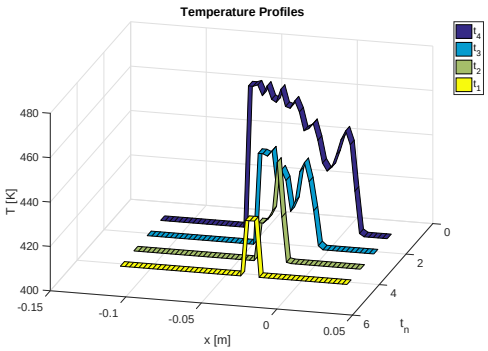

Figure 8: Temperature profiles of the layer adjacent to the lower cylinder.

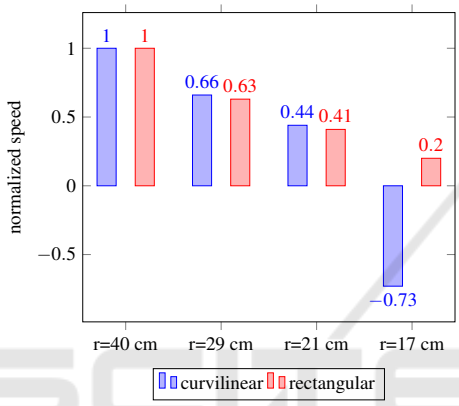

Figure 9: Normalized speed at a point with constant rpm and variable radius of the cylinders.

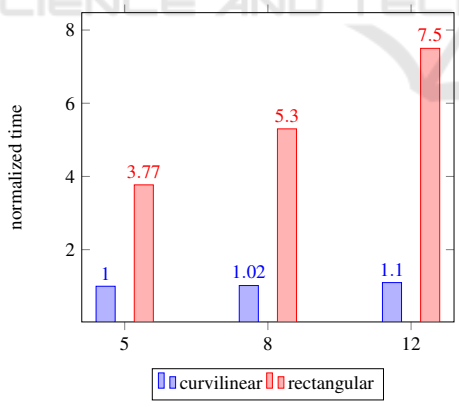

Figure 10: Normalized calculation time of 100000 time steps with 5,8 and 12 calculation nodes at the narrowest gap.

already mentioned before, the high calculation time for the rectangular grid results from the higher number of calculation nodes. In the comparison, the number of calculation nodes in the y-direction for both calculation grids was kept constant at the narrowest gap. Casewise, resulting dimensions for curvilinear grid are 5x50, 8x50 and 12x50, respectiviley 78x50, 136x50 and 215x50 for the rectangular grid. It should be mentioned that the computional time step in both grids is the same. Thus the calculation time is only dependent on the dimension of the grid and not on the time step size as in (Morianou et al., 2016), where the time step size in the rectangular grid is smaller than in the curvilinear grid.

7 CONCLUSIONS

This paper presents a mathematical model of a non-isothermal, high-viscosity fluid that flows between two counter-rotating cylinders. In combination with the MAC method, the model offers the possibility to determine the course of the free surface. For this purpose, the underlying distribution parametric model is discretized with respect to numerical simulation on a curvilinear grid and not, as usual, on a rectangular grid. Since with a curvilinear grid, the edge of the cylinders is identical to the outer lines of the discretizing grid, the system of differential-algebraic equations resulting from the spatial discretization is reduced compared to that of a rectangular grid. However, a sensible use of the curvilinear grid is only possible with sufficiently large radii. Due to the coarser discretization, too small radii typically lead to inaccurate calculation results. The aspect of how an increased radius of curvature exactly affects a numerical error is to be further analysed and the comparison of the quality of both models to measured data on a real system is to take place in more advanced work.

REFERENCES

Aamo, O. M. and Krstic, M. (2003). *Flow Control by Feedback: Stabilization and Mixing*. Springer.

Amsden, A. A. and Harlow, F. H. (1970). The smac method: A numerical technique for calculation incompressible fluid flows. Technical report, Los Alamos Scientific Laboratory of the University of California.

Chorin, A. J. (1968). Numerical solution of the navier-stokes equations. *Mathematics of Computation*, 22(104):745–762.

Dellar, O. J. and Jones, B. L. (2016). Discretising the linearised navier-stokes equations: A systems theory approach. *UKACC International Conference on Control (Control)*.

Harlow, F. H. and Welch, J. E. (1965). Numerical calculation of time-dependent viscous incompressible-flow of fluid with free surface. *The Physics of Fluids*, 8(12):2182 – 2189.

Hirt, C. W. and Shannon, J. P. (1968). Free-surface stress conditions for incompressible-flow calculations. *Journal of Computational Physics*, 2:403 – 411.

Hou, T. Y. and Wetton, B. T. R. (1993). Second-order convergence of a projection scheme for the incompressible navier-stokes equations with boundaries. *Society for Industrial and Applied Mathematics*.

Jones, B. L., Heins, P. H., Kerrigan, E. C., Morrison, J. F., and Sharma, A. (2015). Modelling for robust feedback control of fluid flows. *Journal of Fluid Mechanics*, 769:687–722.

Jovanovic, M. and Bamieh, B. (2001). Modeling flow statistics using the linearized navier-stokes equations. *Conference on Decision and Control*.

McKee, S., Tome, M., Ferreira, V., Cuminato, J., Castelo, A., Sousa, F., and Mangiavacchi, N. (2008). The mac method. *Computer & Fluids*.

Morianou, G. G., Kourgialas, N. N., and Karatzas, G. P. (2016). Comparison between curvilinear and rectilinear grid based hydraulic models for river flow simulation. *Procedia Engineering*, 162:568 – 575.

Nichols, B. D. and Hirt, C. W. (1971). Improved free surface boundary conditions for numerical incompressible-flow calculations. *Journal of Computational Physics*, 8:434–448.

Tome, M., Filho, A., Cuminato, J., Mangiavacchi, N., and McKee, S. (2000). Gensmac3d: a numerical method for solving unsteady three-dimensional free surface flows. *International Journal for Numerical Methods in Fluids*.

Tome, M. F. and McKee, S. (1994). Gensmac: A computational marker and cell method for free surface flows in general domains. *Journal of Computational Physics*, 110:171–186.

Weickert, J. (1996). Navier-stokes equations as a differential-algebraic system. Technical report, Technische Universitt Chemnitz-Zwickau.

Weston, B. (2000). A marker and cell solution of the incompressible navier-stokes equations for free surface flow. Technical report, Department of Mathematics University of Reading.